

Computational Biophysics

RLE Group

Computational Biophysics Group

Academic and Research Staff

Professor Collin Stultz

Graduate Students

Charles Fisher
Elaine Gee
Austin Huang
Paul Nerenberg
Christine Phillips
Ramon Salsas-Escat
Joyatee Sarker
Orly Slavin
Zeeshan Syed

Visiting Graduate Students

Madhavi Gavini
Thomas Gurry

Undergraduate Students

Anjali Muralidhar,
Steven Pennybaker

Collaborators

Prof. Catherine Drennan (MIT Chemistry)
Prof. John Gutttag (MIT, EECS)
Prof. D. E. Ingber (Harvard Medical School)
Prof. Barbara Imperiali (MIT Chemistry)
Prof. Charlie Sodini (MIT, EECS)
Prof. Anantha Chandrakasan (MIT, EECS)

Technical and Support Staff

Arlene Wint

Introduction/Group Overview

The RLE Computational Biophysics Group is focused on understanding conformational changes in biomolecules that play an important role in common human diseases. The group uses an interdisciplinary approach combining computational modeling with biochemical experiments to make connections between conformational changes in macromolecules and disease progression. By employing two types of modeling, molecular dynamics and probabilistic modeling, hypotheses can be developed and then tested experimentally.

1. The Structure of Collagen and Collagenolysis

Sponsors:

National Science Foundation award no. MCB -- 0745638, Burroughs Wellcome Fund Contract no.1004339.01, W.M. Keck Foundation,

Project Staff:

Paul Nerenberg, Prof. Collin Stultz, Thomas Gurry

1.1 The Mechanism of Collagenolysis: A Substrate-centric View

Collagenolysis (collagen degradation) is a critical process in the progression of cancer metastasis, atherosclerosis, and other diseases. Despite considerable efforts to understand the steps involved, the exact mechanism of collagenolysis remains unknown. We have proposed a degradation mechanism in which collagen exists in multiple states, some featuring structures that are unwound in the vicinity of the collagenase cleavage site, and that collagenases preferentially bind to and stabilize the unwound structures before degradation occurs.

The focus of this work is to investigate several aspects of this degradation mechanism using both experimental and computational methods. In particular, we have used molecular dynamics simulations to explore the structure of human type I collagen in the vicinity of the collagenase cleavage site. Simulations of type I collagen in this region suggest that partial unfolding of the $\alpha 2$ chain is energetically preferred relative to unfolding of the $\alpha 1$ chains. Localized unfolding of the $\alpha 2$ chain leads to a metastable structure that has disrupted hydrogen bonds N-terminal to the collagenase cleavage site. Our data suggest that this disruption in hydrogen bonding pattern leads to increased chain flexibility, thereby enabling the $\alpha 2$ chain to sample different partially unfolded states. We are currently testing this hypothesis experimentally by using the catalytic domains of collagenases as a probe for partially unfolded states.

We are also conducting NMR experiments with model peptides of type III collagen, another fibril-forming collagen present in many of the same tissues as type I collagen. The overall goal of these experiments is to quantify the ratio of folded to partially unfolded states in the vicinity of the collagenase cleavage site, as well as in the vicinity of the four pseudo-cleavage sites (i.e., sites that potentially could be cleaved by collagenases, but normally are not). These experiments will enable us to test a related hypothesis that the primary difference between the real cleavage site and the various pseudo-cleavage sites is the extent of unfolding in the vicinity of the scissile bond.

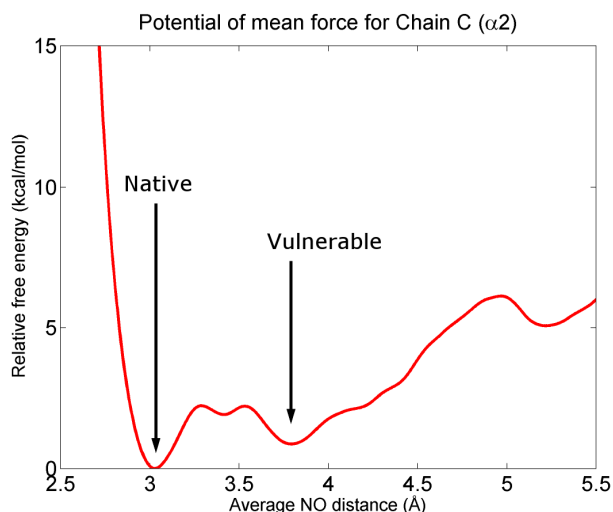
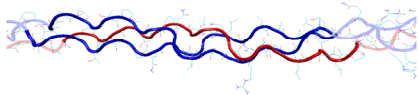
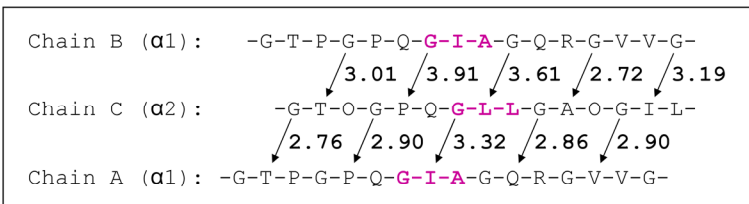


Figure 1: Potential of mean force for chain C ($\alpha 2$) of type I collagen showing both native and vulnerable states.

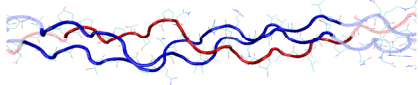
(a)



(b)



(c)



(d)

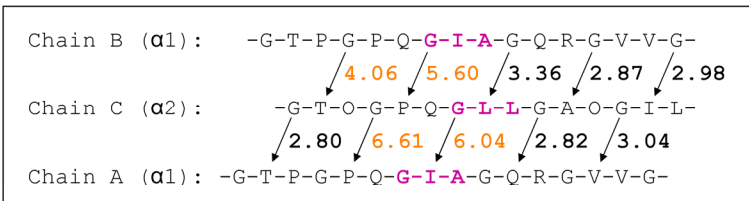


Figure 2: (a) Representative structure from the native state of type I collagen. The $\alpha 2$ chain is colored in red. (b) Interchain NO distances of the native state of type I collagen. The triplets containing the scissile bonds are colored in magenta. (c) Representative structure of the vulnerable state of type I collagen. (d) Interchain NO distances of the vulnerable state of type I collagen. NO distances greater than 4 Å are highlighted in orange.

1.2 The Contribution of Salt Bridges to Triple-Helical Stability

Conformational stability is a critical property of the collagen triple helix. It is in part ensured by the presence of a repetitive GXY sequence motif, with a high frequency of proline residues in the X position and hydroxyproline residues in the Y position. A high natural abundance of lysine residues in the Y position followed by an acidic residue in the following X position also occurs in collagen-like sequences. We hypothesized that these sequences result in inter-chain electrostatic interactions which stabilize the collagen triple helix. To investigate this hypothesis, we performed umbrella sampling molecular dynamics simulations of these sequences hosted in the model peptides $(\text{GPO})_3$ GPKGEO $(\text{GPO})_3$ and $(\text{GPO})_3$ GPKGDO $(\text{GPO})_3$. By constructing potentials of mean force as a function of the inter-chain lysine-N ζ to glutamate-C δ /aspartate-C γ inter-atomic distances, we showed that in all but the chain C to chain A interaction in GPKGDO, energy minima in the potentials of mean force correspond to salt-bridge conformations between the lysine and acidic residues (Figure 1A). At larger inter-atomic distances, where the electrostatic interactions can be considered broken, free energies from the potentials of mean force are significantly higher than those of the salt-bridge states, conclusively showing that these interactions stabilize the triple helical structure of collagen (Figure 1B). These findings suggest that inter-chain salt-bridges could play crucial roles in stabilising collagen triple helices, particular in hydroxyproline-deficient regions and in organisms lacking the prolyl hydroxylase enzyme.

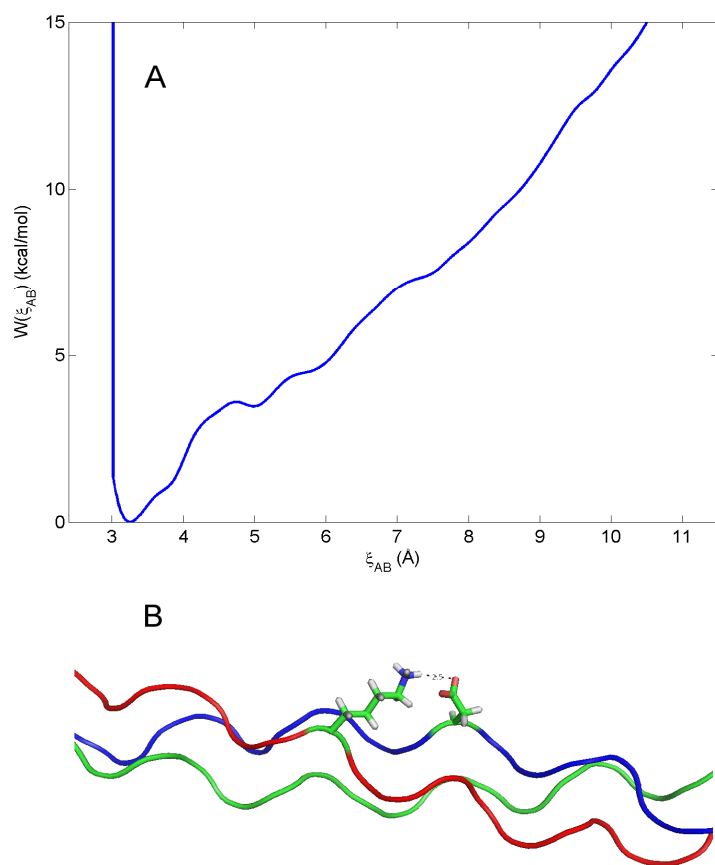


Figure 1 - (A) Potential of mean force for the GPKGDO chain A to chain B interaction. (B) Structural representation of the A-B salt bridge.

2. The Role of Unfolded States in Collagen Degradation

Sponsors:

HST, RLE, Burroughs Wellcome Fund Contract no. 1004339.01, W.M. Keck Foundation, Merck Foundation

Project Staff:

Ramon Salsas-Escat, Prof. Collin Stultz, Steven Pennybaker

2.1 The Role of Unfolded States in Collagen Degradation

Matrix Metalloproteases (MMPs) cleave native collagen at a single site despite the fact that collagen contains more than one scissile bond that can, in principle, be cleaved (Figure 1). For peptide bond hydrolysis to occur at one specific site, MMPs must: 1) localize to a region near the unique scissile bond; 2) bind residues at the catalytic site that form the scissile bond; and 3) hydrolyze the corresponding peptide bond. Prior studies suggest that for some types of collagen, binding of non-catalytic MMP domains to amino-acid sequences in the vicinity of the true cleavage site facilitates the localization of collagenases. In the present study, our goal is to determine whether binding to the catalytic site also plays a role in determining MMP specificity. To investigate this, we computed the conformational free energy landscape of type III collagen at each potential cleavage site (Figure 2). The free energy profiles suggest that while all potential cleavage sites sample unfolded states at relatively low temperatures, the true cleavage site samples structures that are more vulnerable (i.e. the scissile bond is more solvent exposed, Figure 3) and complementary to the catalytic site (they dock best into the active site of an MMP, Figures 4 and 5). By contrast, potential cleavage sites that are not cleaved sample states that are less vulnerable and that are relatively incompatible with the MMP active site. These data imply that locally unfolded potential cleavage sites in type III collagen sample distinct unfolded ensembles, and that the region about the true collagenases cleavage site samples states that are most complementary to the MMP active site.

S1 (757-807)	: GDA-GQO-GEK-GSO-GAQ-GPO-GAO-GPL-G~IA-GIT-GAR-GLA-GPO-GMO-GPR-GSO-GPQ
S2 (766-816)	: GSO-GAQ-GPO-GAO-GPL-GIA-GIT-GAR-G*LA-GPO-GMO-GPR-GSP-GPQ-GVK-GES-GKO
S3 (496-546)	: GDA-GAO-GAO-GGK-GDA-GAO-GER-GPO-G*LA-GAO-GLR-GGA-GPO-GPE-GGK-GAA-GPO
S4 (598-648)	: GPI-GPO-GPA-GQO-GDK-GEG-GAO-GLO-G*IA-GPR-GSO-GER-GET-GPO-GPA-GFO-GAO
S5 (811-861)	: GES-GKO-GAN-GLS-GER-GPO-GPQ-GLO-G*LA-GTA-GEO-GRD-GNP-GSD-GLO-GRD-GSO

Figure 1: Sequence corresponding to the 5 potential cleavage sites in type III collagen. The true collagenase cleavage site (defined by the triplet GIA) is colored in green, while potential cleavage sites (three GLA triplets and one GIA triplet), that are not cleaved, are colored in red. The actual scissile bond is depicted with a ~ sign, while the scissile bonds corresponding to triplets that are not cleaved are depicted with a * sign.

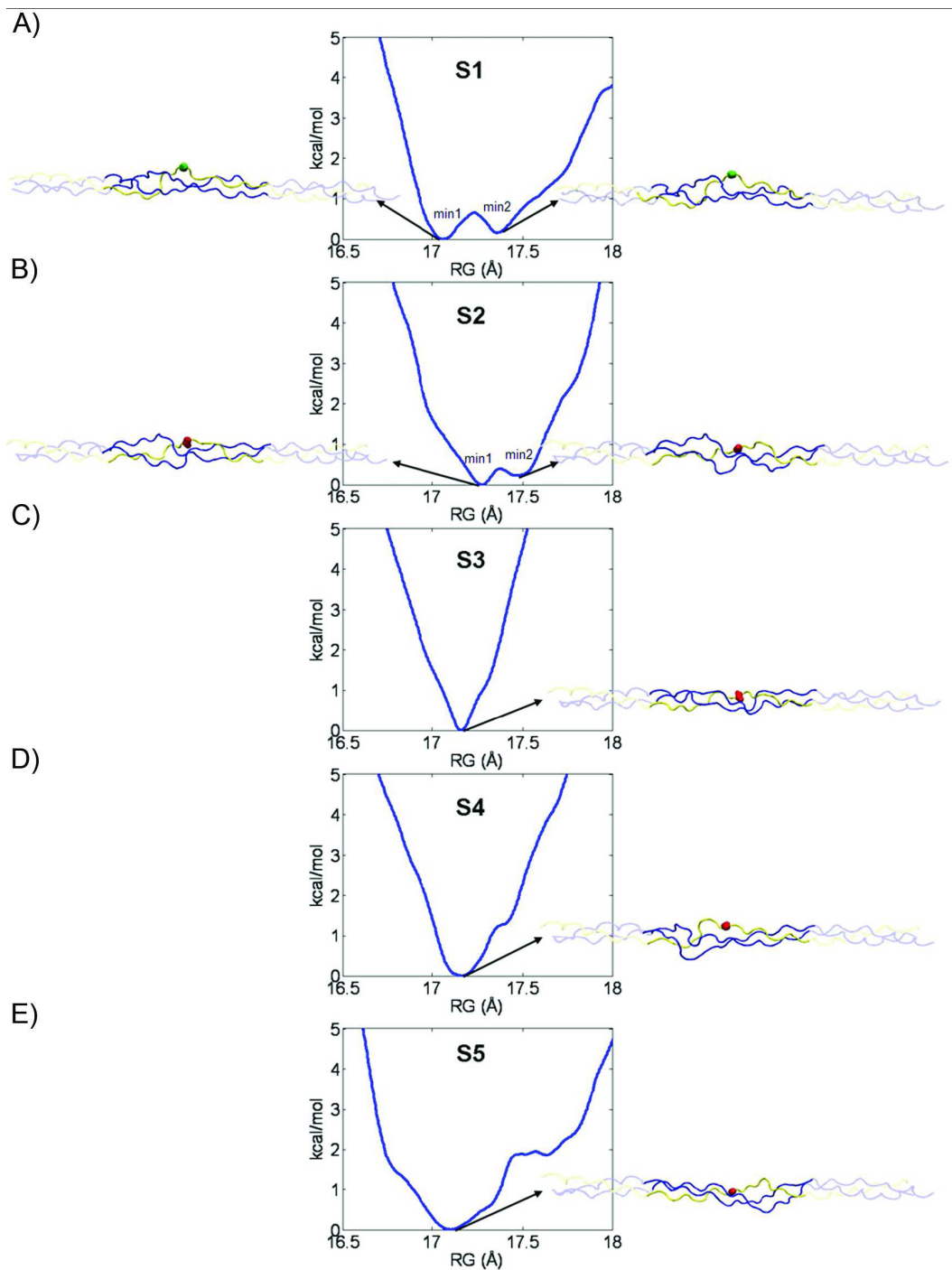


Figure 2: Potential of mean force (pmf) plots for the five potential cleavage sites in type III collagen (sequences listed in Fig. 1). Representative structures from each energy minimum are shown. The four atoms comprising the scissile bond (H, N, C and O) are shown in green for the true cleavage site and in red for the four potential cleavage sites.

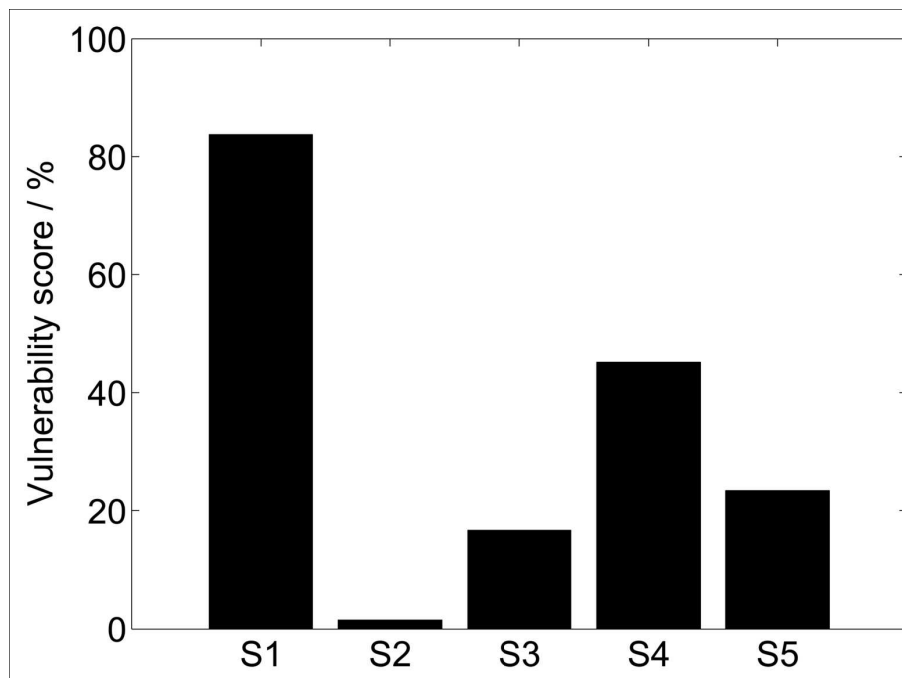


Figure 3: Vulnerability Score plots for the 5 cleavage sites in type III collagen. Vulnerability values are expressed as a percentage, with 100% being the vulnerability of the scissile bond of a G-I or GL dipeptide free in solution.

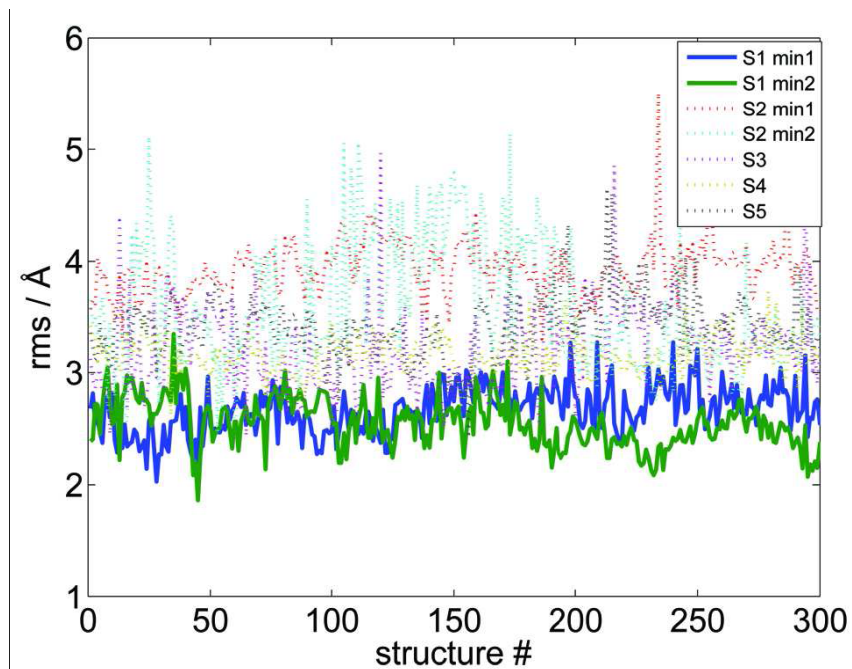


Figure 4: Results of docking studies. RMS values are computed between the backbone atoms of the collagen-like peptide in the co-crystal structure of MMP8 and the corresponding backbone atoms in the chain A of the triple helical peptide. All 300 structures from each energy minimum shown in Figure. 2 were individually docked into CMMP8.

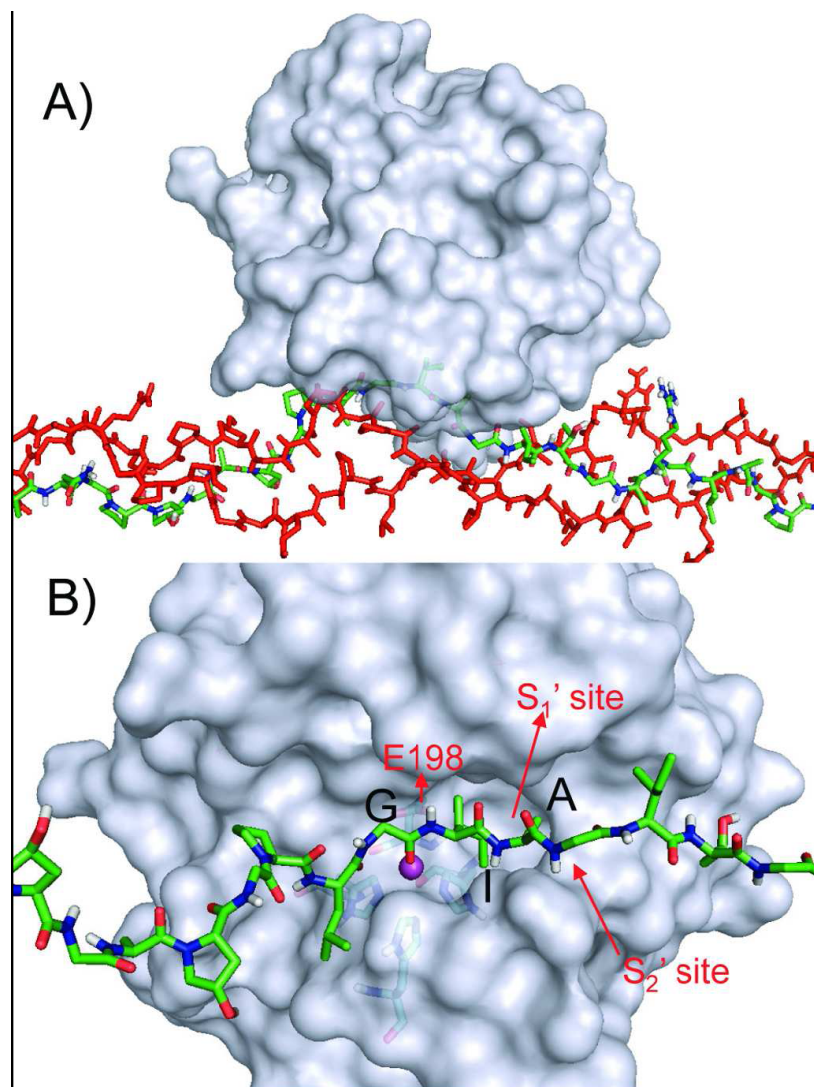


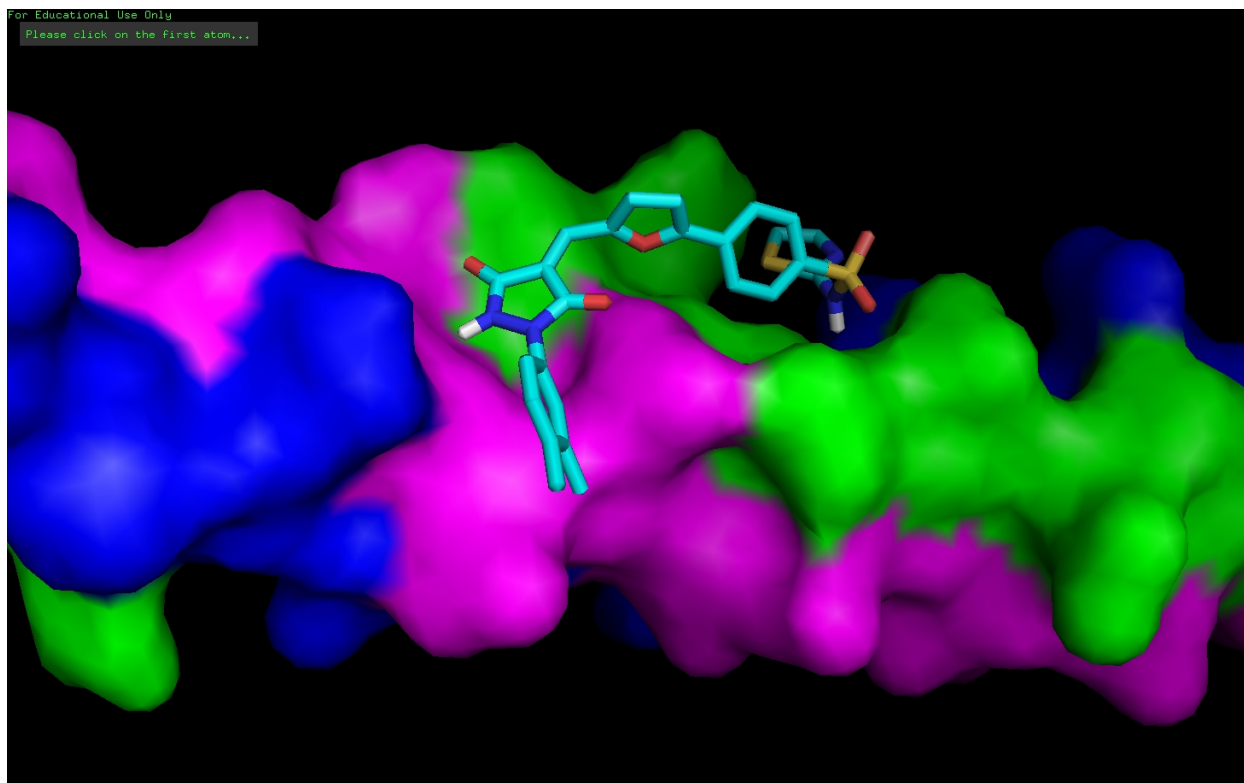
Figure 5: A) Overview of the best docked structure of S1 into the catalytic site of CMMP8. Chain A, which is unfolded in our simulations, is shown in stick representation, while chains B and C are colored in red. The structure of CMMP8 is transparent.

B) The catalytic site of the bound complex with chain A present (chains B and C deleted). The catalytically important E198 is shown, together with the 3 histidine residues that coordinate the Zn⁺² ion. The isoleucine side chain sits in the S1' site, while the alanine side chain sits in the S2' site.

2.2 A Virtual screens for molecules that modulate collagen stability

Triple-helical collagen is the most abundant protein in all mammals. It is hypothesized that naturally, collagen samples partially unfolded states. These states are accessed when one strand partially unwinds from the triple-helix. When in this unfolded state, collagen is susceptible to cleavage by Matrix metalloproteases (MMPs). MMPs play a role in regulating multiple biological functions, but when levels of collagen degradation are abnormally high, they can also play a role in multiple diseases, such as atherosclerosis and cancer. The goal of my work is to find a small molecule which can bind to, and stabilize, collagen in its folded form. I am using AutoDock, a molecular docking simulator, to screen for molecules received from the ZINC database that have this potential and will then be testing them in vitro.

The attached picture is of a potential small molecule bonded to the triple-helical collagen.



3. Modeling the Unfolded State of Tau Protein

Sponsors:

HST, RLE, Jonathan Allen Junior Faculty Award, Westaway Research Fund; NIH R21

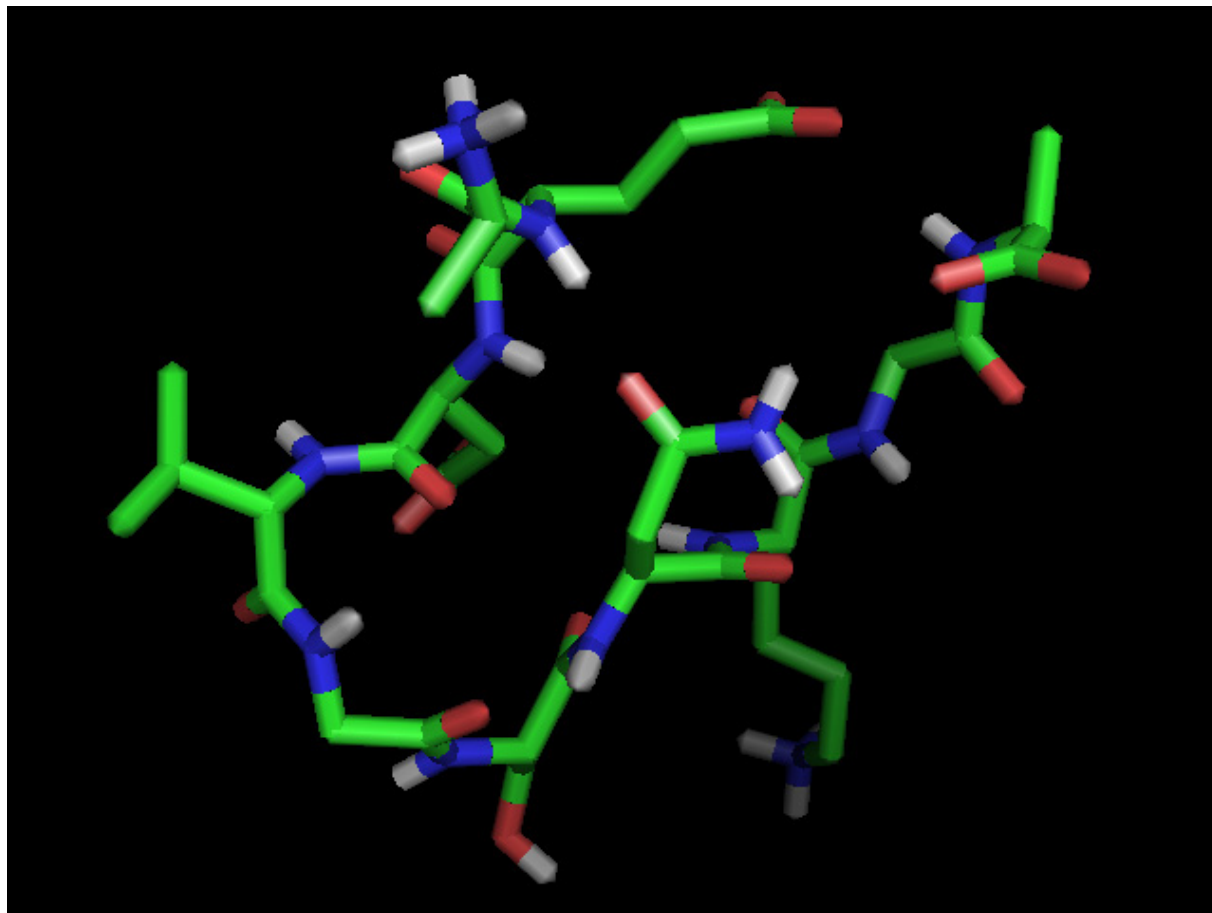
Project Staff:

Madhavi Gavini, Austin Huang, Prof. Collin Stultz

3.1 Title Needed for Madhavi's contribution

I computationally studied the monomeric structure of amyloid beta, a protein that forms amyloid plaques in the brains of individuals with Alzheimers. A library of structures was generated using replica exchange and these structures were then clustered based on potential energy and RMSD to derive a set of representative structures. These structures were then analyzed and their predicted scalar coupling constants and chemical shifts were compared to experimentally derived values to establish a baseline which will be used as a starting point to develop semi-empirical models which may more accurately model theoretical simulations after experimental conditions. I also computationally investigated whether a disorder predicting algorithm, PONDR is effective in predicting intrinsically disordered sites for non-globular proteins that require multiple subunits to form a complete structure. It was found that this algorithm was not as effective in determining disordered sites for linear proteins that require multiple subunits such as collagen.

The attached figure shows one of the representative structures derived using the clustering algorithm developed that takes into consideration both RMSD and energy.



4. Intrinsically Disordered Proteins

Sponsors:

HST, RLE, Burroughs Wellcome Fund Contract no. 1004339.01, Westaway Research Fund, NIH R21

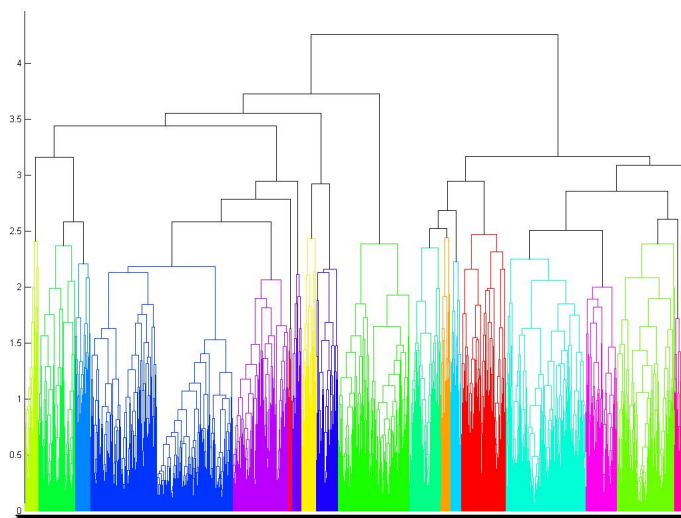
Project Staff:

Orly Slavin, (Veena Venkatachalam), Austin Huang, Prof. Collin Stultz

4.1 Intrinsically Disordered Proteins

Intrinsically disordered proteins (IDPs) comprise a large group of biopolymers that do not adopt well-defined three dimensional structures under physiological conditions. α -Synuclein is one such intrinsically disordered protein that forms organized fibrils composed, mainly of β - structure. The medical significance in studying the α -Synuclein protein is vast. This protein has been implicated in the pathogenesis of several neurodegenerative diseases, including Alzheimer's disease, and Parkinson's disease (PD) associated dementia with Lewy bodies.

We develop structural models of α -Synuclein that accurately represent the ensemble of conformations that are accessible to the protein under physiologic conditions. Our overarching hypothesis is that the unfolded state of IDPs can be modeled as a set of energetically favorable conformations where each conformation corresponds to a local energy minimum on a complex potential energy surface. We construct the conformations that contribute to the ensemble that represent the unfolded state by using a computation method called Energy Minima Mapping that was developed in the Computational Biophysics Group. These ensembles are formed using experimental data such as chemical shifts and residual dipolar coupling. As a first step we used molecular dynamics simulations to construct the multiple possible configurations. We first divide the protein into overlapping segments; following this we find possible conformations for each segment. Last, we use clustering algorithms to combine the segments into possible conformations for the entire protein.



Clustering tree for a representative eight amino acids long segment, using the side chains as a criteria to decide which conformations share spatial similarity

5. Computational Studies of Nickel Regulatory Protein NikR

Sponsors:

HST, RLE, Jonathan Allen Junior Faculty Award, Drennan's

Project Staff:

Christine Phillips, Anjali Muralidhar, Prof. Catherine Drennan, Prof. Collin Stultz

5.1 NikR: A Brief Introduction to the Problem

Regulation of transition metals in the cell is crucial for all living organisms. While some enzymes require metals to function properly, an excess of metal ions in the cell can induce apoptosis. In bacteria, the transcription factor NikR regulates the concentration of nickel ions within the cell. Biochemical studies have shown that *Escherichia coli* NikR binds to DNA with a nanomolar affinity when stoichiometric nickel is present, but with picomolar affinity when excess nickel ions are present (1). Our computational studies aim to determine whether there is a single nickel site or a series of sites that account for the increased affinity and to examine the possible location(s) of these sites.

There are two proposed possibilities for the location(s) of these excess sites. The first possibility is at the interface of the central portion of the structure and the DNA binding portion (shown in Fig. 1 in pink spheres). However, our recently published work shows that this site prefers the cellularly abundant K^+ ion over the divalent Ni^{2+} ion for both electrostatic and size reasons (2).

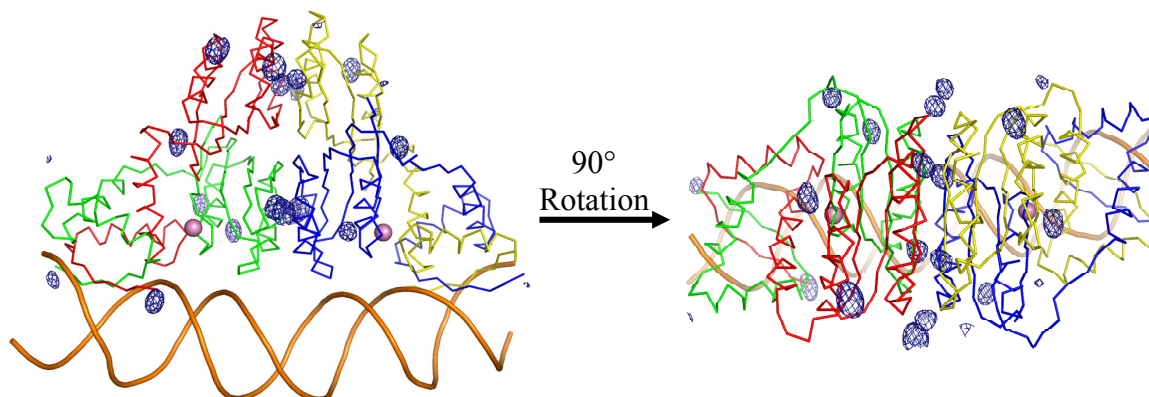


Figure 1. Metal binding sites on NikR. Protein is represented in ribbons in red, green, blue, and yellow with DNA in orange. Extra nickel binding sites on the surface of NikR with nickel ions represented in blue mesh. Potassium ions are shown in pink (3).

Crystallographic studies of EcNikR bound to DNA with excess nickel present indicated that excess nickel ions did not bind in a single specific site, but bound to unconserved histidines on the surface of the protein (Fig. 1) (3). The second proposal for the location of these excess nickel binding sites is at these locations on the surface of the protein (shown in Fig. 1 in mesh). Using Poisson-Boltzmann directed electrostatic computations we will probe these potential excess nickel sites seen in the excess nickel-soaked structure to determine which, if any, of these sites is responsible for the increased NikR-DNA affinity.

Applying computational methods to the excess nickel question

With these calculations, we would like to investigate if the nickel sites on the surface of the protein in the excess-nickel soaked structure can account for the increase in NikR-DNA binding affinity. We will

specifically determine the difference in free energy change upon NikR-DNA binding with stoichiometric nickel (DG_{Stoic}) and NikR-DNA binding with excess nickel (DG_{Excess}) (Fig. 2).

One way to calculate this difference is to determine the change in free energy upon binding DNA with excess nickel (Fig. 2, DG_{Excess}) and similarly with stoichiometric nickel (Fig. 2, DG_{Stoic}). Subtracting these changes in free energy we can determine the effect excess nickel has on DNA binding affinity ($DDG = DG_{\text{Excess}} - DG_{\text{Stoic}}$). We can simplify this calculation using the Poisson Boltzmann formalism and simply calculate the difference in free energy between the stoichiometric and excess nickel-bound states (Fig. 2, DDG). If DDG is negative, then the excess nickel sites we include do increase NikR's affinity for DNA, while a positive DDG value would indicate that nickel binding in these sites does not increase NikR's affinity for DNA.

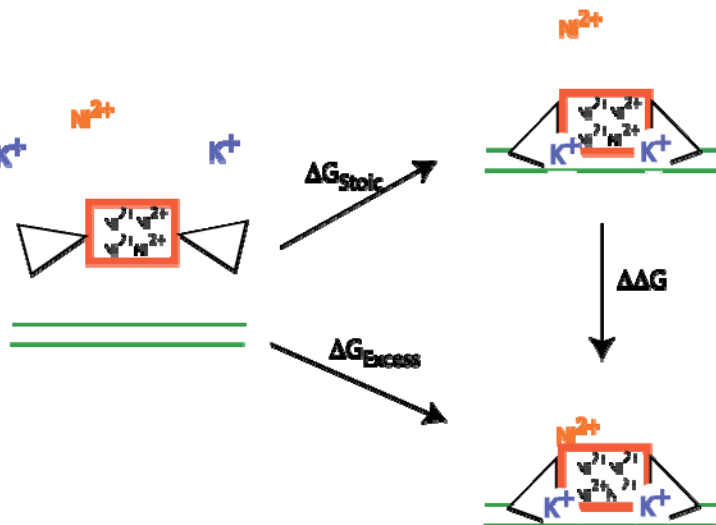


Figure 2. Thermodynamic box illustrating our technique for computational analysis of the effect of the excess nickel binding sites.

From the Poisson Boltzmann calculations we can also determine the impact each amino acid has on the overall free energy difference of the structures and therefore which amino acids may be crucial for explaining the difference in DNA binding affinity of stoichiometric and excess nickel bound NikR.

References

- 1 Bloom, S. L., and Zamble, D. B. (2004) Metal-Selective DNA-Binding Response of *Escherichia coli* NikR, *Biochemistry* 43, 10029-10038.
- 2 Phillips, C. M., Nerenberg, P. S., Drennan, C. L., and Stultz, C. M. (2009) Physical Basis of Metal-Binding Specificity in *Escherichia coli* NikR, *J Am Chem Soc* 131, 10220-10228.
- 3 Schreiter, E. R., Wang, S. C., Zamble, D. B., and Drennan, C. L. (2006) NikR-operator complex structure and the mechanism of repressor activation by metal ions, *Proc. Natl. Acad. Sci. U. S. A.* 103, 13676-13681.
- 4 Honig, B., and Nicholls, A. (1995) Classical Electrostatics in Biology and Chemistry, *Science* 268, 1144-1149.
- 5 Norberg, J. (2003) *Archives of Biochemistry and Biophysics* 410, 48-68.

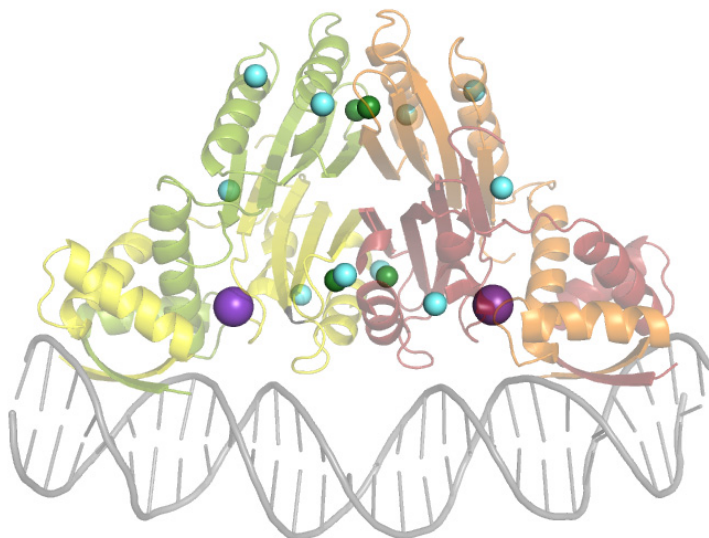
Our recent publications on NikR:

Phillips, C.M., Nerenberg, P.S., Drennan, C.L. and Stultz, C.M. Physical Basis of Metal-Binding Specificity in *Escherichia coli* NikR. *Journal of the American Chemical Society* (2009) **131**, 10220-10228.

5.2 Investigating the role of excess nickel sites in NikR regulation

I computationally investigated the effects of various factors that can reduce the amount of collagen degradation that occurs. It was found that the introduction of an enzyme inhibitor, which will have a high affinity for collagenases prevent collagenases from binding to collagen and causing cleavage, can reduce degradation at a lower energy than a molecule that will stabilize collagen in its triple helical state and prevent cleavage. However, it is unclear whether the computationally determined binding energies of the stabilizing molecule and enzyme inhibitor are realistically achievable. I have also been computationally analyzing the structure of the regulatory transcription factor, NikR, which regulates the amount of nickel in a cell. In particular, I have been investigating the structure of NikR in the presence of excess nickel ions that fill low affinity sites at the surface of the protein. These low affinity sites may be the reason for increased affinity of NikR for DNA in the presence of excess nickel.

The figure below shows NikR, with potassium ions (purple) stabilizing the NikR-DNA complex, nickel ions in high affinity sites near the center of the protein (green), and nickel ions in low affinity sites around the surface of the protein (light blue).



6. Understanding Fibronectin Fibrillogenesis by Modeling Physiologic Unfolding of Fibronectin with Steered Molecular Dynamics Simulation

Sponsors:

NIH (Award No.s NIH/NIGMS Molecular Biophysics Training Grant T32 GM008313 and NIH CA45548), Keck Foundation (NAKFI Nano 06), Harvard Materials Research Science and Engineering Center, Department of Defense Innovator Award No. W81XWH-08-1-0659, RLE, Burroughs Wellcome Fund Contract no. 1004339.01

Project Staff:

Elaine Gee, Prof. D.E. Ingber, Prof. Collin Stultz

6.1 Cell-Mediated Fibronectin Unfolding

When a particular Fibronectin (FN) polymerization is essential for the development and repair of these computational simulations.

The extracellular matrix (ECM) controls cell behavior by affecting adhesion, migration, gene expression, proliferation, and survival through biochemical and mechanical cues. The mature ECM develops from a provisional fibronectin (FN) matrix, which other ECM molecules, such as collagen, require for deposition. The process of FN assembly, or FN fibrillogenesis, plays an important role in ECM formation and function during the development and repair of the extracellular matrix in physiological processes such as embryogenesis, migration, angiogenesis, and wound healing as well as in pathological conditions as in cancer. The process of FN assembly requires both integrin binding to FN as well as cell contractility, which confers strain to the attached molecule. The 10th repeat of FN domain type III (10FNIII) contains the integrin-binding sequence RGD and has been shown to be mechanically weak. However, the role of this module in the molecular process of fibrillar assembly remains unclear. By studying the mechanism by which FN transduces cell-traction forces into the biochemical process of matrix assembly, one can understand the mechanical principles that define the cell microenvironment. The goal of this project is to understand how structural unfolding of 10FNIII by traction force affects FN mechanotransduction.

Data suggest that FN fibrillogenesis is facilitated by cell traction forces (on the order of nNs) transferred to FN via bound membrane integrin receptors. Forces applied to distinct regions of FN drive the formation of partially unfolded FN intermediates that then bind to additional FN molecules. Past studies have focused on FN unfolding by applying pulling force at the N- and C-termini of protein fragments rather than at the site of cell binding. However, since cell membrane integrins bind FN at a surface-exposed RGD loop on 10FNIII, we investigate the mechanism of cell-mediated FN unfolding by using steered molecular dynamics to apply tensile force at the RGD site. While pulling at the N- and C-termini of 10FNIII leads to unfolding trajectories that sample different unfolding pathways as previously published, we find that pulling at the RGD site unfolds 10FNIII along one well-defined pathway. This pathway accesses a partially unfolded intermediate structure with solvent exposed hydrophobic N-terminal residues. Moreover, additional unfolding of this intermediate triggers an arginine residue, which is required for high affinity cell binding, to separate from the adjacent RGD loop. Based on these results, we propose a mechanism by which cell traction induces a conformational change in FN that possibly enables FN-FN associations and cell detachment, thereby promoting the binding of new FN to the cell surface receptor to promote subsequent cycles of adhesion, unfolding, and fibril formation that drive FN matrix assembly (Figure 1). Currently, investigations are underway to provide experimental support for the proposed mechanism obtained from these computational simulations using biophysical approaches including force spectroscopy techniques and cell-based fluorescence assays.

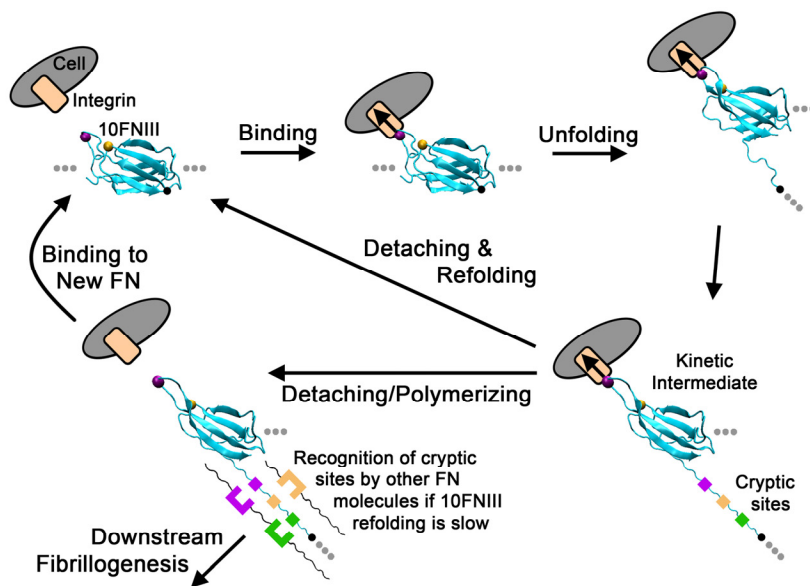


Figure 1. Cell-mediated Fibrillogenesis. The proposed model involves the formation of a partially unfolded intermediate during cell-traction mediated unfolding. Potential cryptic sites that promote FN aggregation and fibrillogenesis may exist in this partially unfolded structure. Subsequent unfolding past this intermediate induces the movement of a crucial arginine (gold bead) at a secondary binding site to a position far from the RGD loop (magenta bead labels the central glycine). This frees the cell from the RGD ligand and enables it to reattach to another FN molecule to propagate the process. If 10FNIII refolding is relatively slow, then unfolded portions of this domain are available to make contacts with other FN molecules to stimulate downstream fibrillogenesis.

Publications:

Gee EPS, Ingber DE, Stultz CM (2008) Fibronectin Unfolding Revisited: Modeling Cell Traction-Mediated Unfolding of the Tenth Type-III Repeat. PLoS ONE 3: e2373.

7. ECG Markers to Predict Cardiovascular Death

Sponsors:

HST, RLE, Westaway Research Fund, CIMIT

Project Staff:

Joyatee Sarker, (Zeeshan Syed), Prof. Collin Stultz, Prof. John Guttag

7.1 ECG Measures to Predict Cardiovascular Outcomes

Patients who have had an acute coronary syndrome (ACS) are at a relatively high risk of having subsequent adverse cardiac events. Several electrocardiographic measures such as heart rate variability, heart rate turbulence, deceleration capacity, and T-wave alternans have been used to identify patients at increased risk of adverse cardiac events. An algorithm called dynamic time warping (DTW) aligns heart beats to minimize differences, producing a morphologic distance (MD) time series. The irregularities in the MD time series are measured as the morphologic variability (MV). Using holter-ECG data from patients who were recently admitted with an ACS, we are determining whether morphology based measures can be used to identify patients at high risk of other adverse cardiac events, such as congestive heart failure, recurrent ischemia and myocardial infarction.

	<i>Coefficients</i>	<i>P-value</i>
age	0.0017	2.33E-06
female	0.0064	0.3608
bmi	0.0002	0.7325
history of diabetes	0.0143	0.0388
history of hypertension	-0.0008	0.9173
current smoker	0.0112	0.1531
prior MI	0.0218	0.0020
history of CHF	0.0080	0.3684
ST segment depression	0.0081	0.2221
SDNN < 50ms	0.0114	0.6249
SDANN < 40ms	-0.0379	0.1301
HRVI < 20U	0.0171	0.0291
HRV-LF/HF > 0.95	0.0353	3.02E-05
LVEF < 40%	0.0452	7.29E-06
MV > 52.5	0.0048	0.5782

Association between clinical and ECG variables and future CHF using a multivariate model.

Patients who died were not included in this model. Significant p-values (< 0.05) are bolded.

Publications

Journal Articles, Published

C. Phillips, P. Nerenberg, C. Drennan, C.M. Stultz, "The Physical Basis of Metal Binding Specificity in *E. coli* NikR," *Journal of the American Chemical Society* 131(29): 10220-10228 (DOI: 10.1021/ja9026314), (2009).

C. Schubert, and C.M. Stultz, "The Multi-Copy Simultaneous Search Methodology: A Fundamental Tool for Structure-Based Drug Design," *Journal of Computer Aided Molecular Design* (DOI: 10.1007/s10822-009-9287-y), (2009).

A. Huang, and C.M. Stultz, "Finding Order within Disorder: Elucidating the Structure of Proteins Associated with Neurodegenerative Disease," *Future Medicinal Chemistry* 1(3): 467-482, (2009).

Z. Syed, P. Sung, B.M. Scirica, D.A. Morrow, C.M. Stultz, and J.V. Guttag, "Spectral Energy of ECG Morphologic Differences to Predict Death," *Cardiovascular Engineering* (DOI 10.1007/s10558-009-9066-3), (2009).

M. Yoon, V. Venkatachalam, A. Huang, B. Choi, C.M. Stultz, and J.J. Chou, "Residual Structure within the Disordered C-Terminal Segment of p21Waf1/Cip1/Sdi1 and its Implications for Molecular Recognition," *Protein Science* 18(2): 337-347, (2009).

Z. Syed, P. Sung, B.M. Scirica, S. Mohanavelu, P. Sung, C.P. Cannon, P.H. Stone, C.M. Stultz, and J.V. Guttag, "Relation of Death within 90 days of Non-ST-Elevation Acute Coronary Syndromes to Variability in Electrocardiographic Morphology," *American Journal of Cardiology*, 103(3): 307-311 (DOI: 10.1016/j.amjcard.2008.09.099), (2009).

A. Huang, and C.M. Stultz, "The Effect of a Δ K280 Mutation on the Unfolded State of a Microtubule-Binding Repeat in Tau," *PLoS Computational Biology* 4(8): e1000155 DOI:10.1371/journal.pcbi.1000155.

P.S. Nerenberg, and C.M. Stultz, "Differential Unfolding of α 1 and α 2 chains in Type I Collagen and Collagenolysis," *JMB* 382, 246-256, (2008).

R. Salsas-Escat, and C.M. Stultz, "Conformational Selection and Collagenolysis in Type III Collagen," *Proteins: Structure, Function, and Bioinformatics* (Accepted article online: Jul 20, 2009) (DOI: 10.1002/prot.22545).

Journal Articles, Accepted for Publication

Z. Syed, C.M. Stultz, M. Kellis, P. Indyk, and J. Guttag, "Motif Discovery in Physiological Datasets: A Methodology for Inferring Predictive Elements," *ACM Transactions on Knowledge Discovery from Data* (In press).

Journal Articles, Submitted

Gurry T., Nerenberg PS, Stultz CM, The Contribution of Salt Bridges to Triple-Helical Stability. Under review.